iJETRM
International Journal of Engineering Technology Research & Management
Published By:
https://www.ijetrm.com/

OPTICAL AND FERROELECTRIC PROPERTIES OF $Pb_{0.4}La_{0.4}Co_{0.2}TiO_3$ NANOPARTICLES

N. SURESH KUMAR
Assistant Professor, Department of Physics, JNTUA College of Engineering Anantapur, Andhra Pradesh, India

P. ANKOJI
Assistant Professor, Department of Physics, JNTUA College of Engineering Pulivendula, Andhra Pradesh, India

B. PRADEEP RAJU
Assistant Professor, Department of Chemistry, JNTUA College of Engineering Anantapur, Andhra Pradesh, India

R. PADMA SUVARNA
Professor, Department of Physics, JNTUA College of Engineering Anantapur, Andhra Pradesh, India

ABSTRACT
The sol-gel method that was processed in a microwave heating was used to create the $Pb_{0.4}La_{0.4}Co_{0.2}TiO_3$ samples. Lead titanate and lanthanum cobalt titanate structure-related tetragonal phases were identified by the diffraction pattern. The existence of metal oxide bonding was determined using the Fourier transform infrared spectra. Additionally, it was determined that the wide optical band gap energy (E_g) was 3.20 eV. Ferroelectric characteristics were also examined in relation to frequency.

Keywords:
Nanoparticles; Microwaves; Diffraction; Ferroelectric; Optical Band Gap

INTRODUCTION
Nanotechnology has become a very useful field for studying the physical, electrical, magnetic, and visual features of nanomaterials (NMs). The nanoscale has become a big part of this. Nanomaterials, on the other hand, are more important than solid materials in pharmacology, biotechnology, and many other technical fields because of their possible electromagnetic and optical qualities [1]. The truth is that these nanomaterials, whether they are magnetic or not, could be very useful in many areas, such as drug delivery systems, data storage devices, superparamagnetic, magnetic hyperthermia, magnetic tapes, magnetic recording, magnetic resonance imaging (MRI), electromagnetic shields, microwave absorbers, dielectric absorbers, and transformer-inductor core devices [1]. Also, it's important to explain how nanomaterials are categorized. In particular, the NMs were put into different groups based on their surface shape, size, and chemical properties [2]. These groups included carbon-based NMs (also known as carbon nanotubes or CNTs), metallic NMs (Au-nanoparticles), ceramic NMs (inorganic nonmetallic solids), semiconductor NMs (also known as wide band gap semiconductors), polymeric NMs (nanospheres and nanocages), and lipid-based NMs (nanospheres). Most of the time, each of the above NMs has its own uses. This study, on the other hand, looks at how to make PLCT nanofibers using the microwave sol-gel method, even though a lot of other research has been focused on making nanofibers using the more expensive electrospinning method. More specifically, these nanofibers have many uses in drug delivery systems because they make it easy to add bioactive growth factors directly to supports [4-6].

International Journal of Engineering Technology Research & Management
Published By:
https://www.ijetrm.com/

EXPERIMENTAL PROCEDURE

The nanomaterials in this investigation were prepared using the sol-gel technique, and the experimental procedure is nearly identical to that reported in other studies [7]. First, a sensitive digital weighing balance was used to weigh the raw elements in accordance with their stoichiometric ratio. Glacial acetic acid was employed as the solvent, and the starting components were selected based on the stoichiometric ratio. A magnetic stirrer was used to carefully mix the glacial solution in a beaker. After Pb(CH3CoO)2 was completely dissolved, further ingredients were added. Throughout the procedure, the temperature was maintained at 323 K. About half an hour later, Ti(OC4H9) was continuously added with a dropper, drop by drop. For one hundred and twenty minutes, the entire solution was left to fully mix. The ethanol and water solution was added to the aforementioned solution using a burette. Moreover, a gel-like solution was produced. After 48 hours of natural drainage, this gel was heated for approximately an hour. This produced a hard crystal that was ground into a fine powder. The resulting powder was then sintered for forty-five minutes at 1023 K in a microwave furnace. The crystalline powder was again ground into a fine powder following sintering. Additionally, the samples were described using a variety of characterization methods for their ferroelectric, morphological, and structural characteristics.

RESULTS AND DISCUSSION

3.1 Structural Ananlysis

Fig. 1 showed the synthesized materials' X-ray diffraction patterns. Figure 1 made it clear that all of the nanoparticles' reflection planes match the typical tetragonal phases of cobalt lanthanum titanate (JCPDS: 89-7505) and lead titanate (PT) (JCPDS: 78-0298). The XRD pattern showed no additional contaminant peaks. Overall, the diffraction pattern analysis revealed a wide range of diffraction peak widths, which may indicate the presence of nanoscale crystallites. In the end, it is clear from the diffraction pattern analysis section that the structure development was significantly impacted by the higher concentrations.

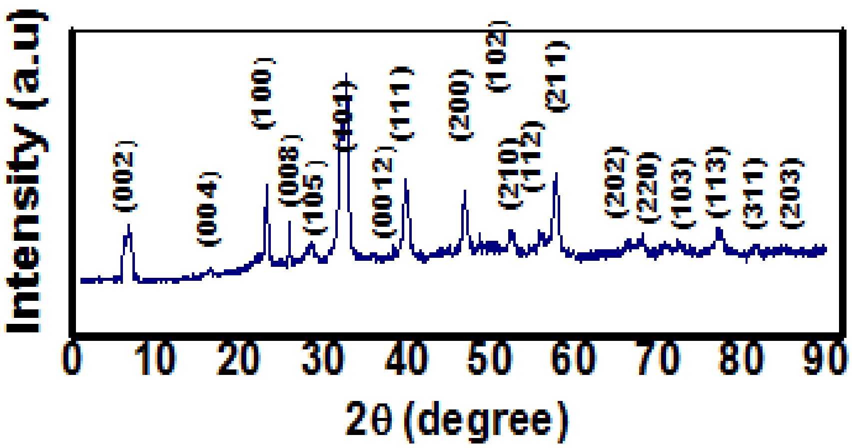

Fig.1. XRD Pattern

3.2 FTIR spectral analysis

As seen in Fig. 2, the produced nanoparticles' FTIR spectra were captured between 4000 and 400 cm^{-1}. The FTIR spectra are often highly helpful in determining the presence of functional groups, stretching vibrational frequencies, and metal oxide bonds (M-O). Fig. 2 made it clear that the wave numbers of the metal oxide bonds at the A-site (υ_1) and B-site (υ_2) varied between around 400 and 500 cm^{-1}. It might be explained by titanium

iJETRM
International Journal of Engineering Technology Research & Management
Published By:
https://www.ijetrm.com/

cations solely occupying the B-site. Shannon had already proposed a similar type of cationic occupancy in the literature [8]. All things considered, this proved that metal oxide bonds like Pb-O, Co-O, and La-O can form at the A-site, but Ti-O bonds can form at the B-site. The bending vibrations of oxygen and hydrogen (O-H) were shown by the FTIR spectra, which displayed distinct absorption bands at about 1354 and 1489 cm^{-1} [9]. Furthermore, the O-H stretching and bending vibrations of H_2O molecules absorbed by nanoparticles, respectively, caused the peaks that developed at approximately 1633 cm^{-1} and 3303 cm^{-1} and 3612 cm^{-1} [10, 11].

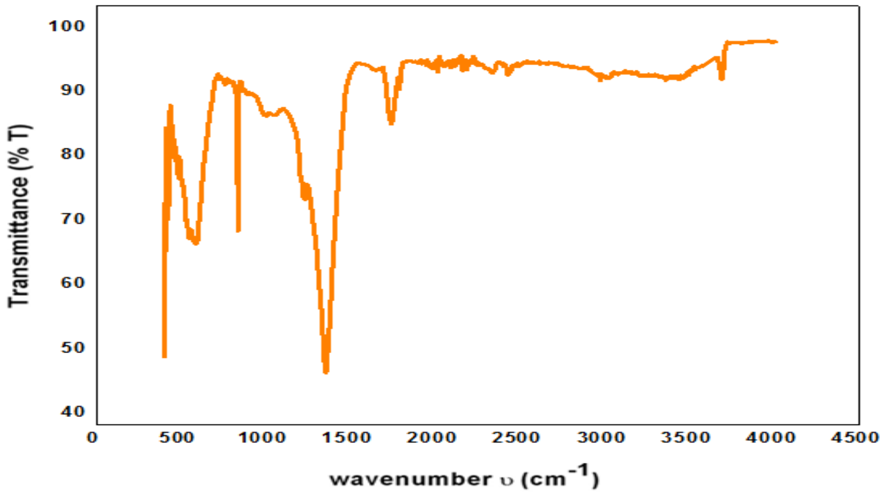

Fig.2. FTIR spectra

3.3 UV-Visible Spectral Analysis

The optical band gap energy (E_g) was determined by extrapolating the linear part of the curve in the direction of photon energy (hv), where the absorption coefficient "α" precisely reached zero. The $(\alpha h\nu)^2$ vs photon energy (hv) graphs in Figure 3 demonstrated it. There appeared to be almost equal direct band gap (3.2 eV). Previous reports in the literature [5] identified this type of band gap based on the cationic exchange between A and B-sites. In rare instances, microwave heating may also be to blame for this sort of behavior. On the other hand, materials with both narrow and large optical band gaps can be used in sensor, photocatalytic, and optoelectronic devices [12, 13].

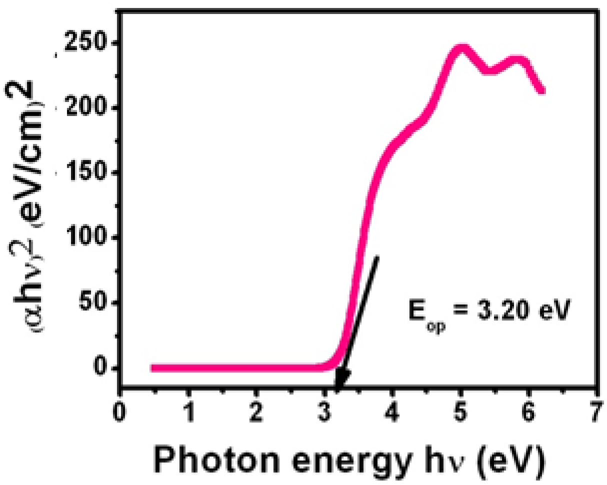

Fig.3 $(\alpha h\nu)^2$ versus photon energy (hv) plot

iJETRM
International Journal of Engineering Technology Research & Management
Published By:
https://www.ijetrm.com/

Ferroelectric Properties

Polarization versus electric field (P-E) loops were used to test the produced nanoparticles' ferroelectric properties. The P-E loops at room temperature were depicted in Fig. 4. The prepared sample's clearly defined hysteresis loop was seen. According to the findings, the saturation polarization Ps value was found to be approximately constant at 0.039 μC/cm^2. This suggested that because charge carriers responded to the applied external ac electric field nearly equally, there was no discernible change in the P_s value for any of the samples. Furthermore, in rare instances, the tiny value of polarization may be caused by current leakage and the oxygen vacancies that occur [4]. Similarly, it was discovered that the remanence polarization (P_r) was 0.039 μC/cm^2. A tiny magnitude of 0.013 μC/cm^2 was displayed. It was observed that the coercive electric field (E_c) was changing from 0.67 kV/cm. As a result, ferroelectric capacitors and ferroelectric memory applications may anticipate these materials [14].

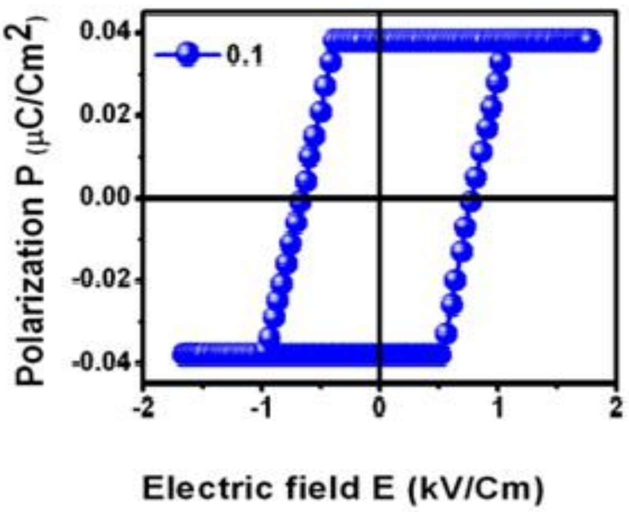

Fig.4. P-E loops of PCLT nanomaterials

CONCLUSION

The sol-gel method was used to create the $Pb_{0.4}La_{0.4}Co_{0.2}TiO_3$ nanoparticles. In addition to a small amount of tetragonal lead titanate (PT) phases, the PCLT nanoparticles also showed cubic phases. The existence of Pb-O, Co-O, La-O, and Ti-O metal oxide bonds at sites A and B was shown by the FTIR analysis. By analyzing UV-visible spectra, the optical band gap energy (E_g) was found to be 3.20 eV. The ferroelectric hysteresis loops were then recorded, showing that the materials had substantial ε' values in magnitude and high E_c values. As a result, ferroelectric capacitors and ferroelectric memory applications are probably suitable for these materials.

REFERENCES

[1]. Wenk, Hans-Rudolf; Bulakh, Andrei. Minerals: Their Constitution and Origin. New York, NY: Cambridge University Press. 2004, ISBN 978-0-521-52958-7.

[2]. C. J. Lu, S. B. Ren, H. M. Shen, J. S. Liu, and Y. N. Wang, Microstructure, composition, and optical properties of $PbTiO_3$ thin films prepared by the sol-gel method, Journal of Vacuum Science & Technology A 15 (1997) 2167

iJETRM
International Journal of Engineering Technology Research & Management
Published By:
https://www.ijetrm.com/

[3].**S.Jachalke**, **E.Mehner**, **H.Stöcker**, **J.Hanzig**, **M.Sonntag**, **T.Weigel**, **T.Leisegang** and **D.C. Meyer**, How to measure the pyroelectric coefficient?, Applied Physics Reviews 4 (2017) 021303

[4]. N. S. Kumar, R. P. Suvarna and K.C. B. Naidu, Phase Change and Ferroelectric Nature of Microwave Heated Lead Cobalt Titanate Nanoparticles Prepared by Sol-Gel Method, International Journal of Applied Ceramic Technology (2018) 1-8, DOI: 10.1111/ijac.13056

[5]. Subhasis Roy and S. B. Majumder, Optical characteristic of sol-gel synthesized lead lanthanum titanate-cobalt iron oxide multiferroic composite thin film, Journal of Applied Physics 112 (2012) 043520

[6]. N. S. Kumar, R. P. Suvarna and K. C. B. Naidu, Sol-Gel Synthesized and Microwave Heated $Pb_{0.8-y}La_yCo_{0.2}TiO_3$ (y= 0.2–0.8) Nanoparticles: Structural, Morphological and Dielectric Properties, Ceramics International (2018), https://doi.org/10.1016/j.ceramint.2018.07.027

[7]. B. D. Cullity, Elements of X-ray diffraction, 2nd ed. (Addison-Wesley, Reading, MA, 1978)

[8]. R.D. Shannon, Revised Effective Ionic Radii and Systematic Studies of Interatomic Distances in Halides and Chalcogenides, *Acta Cryst.* **A 32** (1976) 751-767.

[9].D. Kothandan, R.J. Kumar, M. Prakash, K.C.B. Naidu, Structural, morphological and optical properties of $Ba_{1-x}Cu_xTiO_3$ (x = 0.2, 0.4, 0.6, 0.8) nanoparticles synthesized by hydrothermal method, Materials Chemistry and Physics 215 (2018) 310–315

[10]. Kumar N S, Suvarna R P, Naidu K C B, Structural and ferroelectric properties of microwave heated lead cobalt titanate nanoparticles synthesized by sol–gel technique, J Mater. Sci: Mater. Electron 29 (2018) 4738-4742.

[11]. D. Kothandan, R. J. Kumar & K. C. B. Naidu, Barium titanate microspheres by low temperature hydrothermal method: studies on structural, morphological, and optical properties, Journal of Asian Ceramic Societies 6 (2018) 1-6

[12].Sudharshan Vadnala, Nirupam Paul, Amit Agrawal, S.G. Singh, Enhanced infrared sensing properties of vanadium pentoxide nanofibers for bolometer application, Materials Science in Semiconductor Processing 81 (2018) 82-88

[13].V. Sabaghi, F. Davar and Z. Fereshteh, ZnS nanoparticles prepared via simple reflux and hydrothermal method: optical and photocatalytic properties, Ceram. Inter. 44 (2018) 7545-7556

[14]. I. Zouaria, Z. Sassib, L. Seveyratb, N. Abdelmoulaa, L. Lebrunb, H. Khemakhem, Structural, dielectric, piezoelectric, ferroelectric and electro-caloric properties of $Ba_{1-x}Ca_xTi_{0.975}(Nb_{0.5}Yb_{0.5})_{0.025}O_3$ lead-free ceramics, Ceramics International 44 (2018) 8018-8025